PHYSICAL REVIEW B **75**, 100102(R) (2007)

He diffusion in irradiated α-Fe: An *ab-initio*-based rate theory model

C. J. Ortiz* and M. J. Caturla
Departamento de Física Aplicada, Universidad de Alicante, 03690 San Vicente del Raspeig, Spain

C. C. Fu and F. Willaime
Service de Recherches de Métallurgie Physique, CEA/Saclay, 91191 Gif-sur-Yvette, France

(Received 12 February 2007; revised manuscript received 8 March 2007; published 26 March 2007)

The diffusion of He in irradiated α-Fe is studied using a rate theory model addressing the effect of impurities. *Ab initio* values for the migration and binding energies of He, He-vacancy complexes, vacancy, and self-interstitial clusters are used to model desorption experiments of He-implanted α-Fe. Using the brute *ab initio* data yields a significant discrepancy with experimental measurements. On the other hand, good agreement is obtained when the vacancy migration energy is increased from the original *ab initio* value while the binding energies of vacancies with substitutional and interstitial helium are lowered. The presence of impurities, with carbon being the most likely candidate, is proposed as a justification for these effective energies. Our simulations also provide a detailed description of the diffusion mechanisms of He active under these particular experimental conditions.

DOI: 10.1103/PhysRevB.75.100102 PACS number(s): 61.80.Az, 61.82.Bg, 66.30.−h, 61.72.Ji

Understanding the effect of He in metals is crucial for the development of materials resistant to radiation under fusion and fission conditions.[1] The basic He migration mechanisms are well known,[2–5] but the complexity of the problem is such that there are still many unknowns regarding He migration in the presence of defects.[6] Modeling the evolution of He and the nucleation of He-vacancy complexes requires the coupling between different simulation methods to reach the relevant time and length scales. The use of *ab initio* calculations, to obtain basic parameters such as migration and binding energies of defects, in combination with other models, such as kinetic Monte Carlo or rate theory, has proven to be a successful method to study defect diffusion and clustering both in metals[7–10] and in semiconductors.[11]

Based on recent *ab initio* calculations on the stability and mobility of He-vacancy complexes in Fe,[12,13] we have developed a kinetic model to follow the evolution of defects produced during irradiation of Fe in the presence of He. This model allows us to compare directly with experimental observations, providing information about the role of the different migration mechanisms, as well as the initial stages of nucleation of He-vacancy clusters, precursors of bubbles and voids. The basic types of defects included in the model are self-interstitials (I), vacancies (V), and He atoms. The latter can be at a substitutional site (in which case it is denoted here as a HeV complex) or at an interstitial site (He_i). In this model single vacancies, single self-interstitials, di-interstitials, and He_i are considered to be mobile. All other defects are considered to be immobile. Migration energies of 0.06, 0.67, 0.34, and 0.42 eV obtained by *ab initio* calculations[10,12] for He_i, V, I, and I_2, respectively, were used in this model. By binary reactions, presented below, mobile defects can interact to form more complex ones, such as clusters of interstitials or vacancies (I_n, V_n), where n is the number of defects in a cluster, or clusters of n-He atoms and p vacancies ($\mathrm{He}_n V_p$):

$$\mathrm{He}_i + V \rightleftharpoons \mathrm{He}V, \tag{1}$$

$$\mathrm{He}V + I \rightleftharpoons \mathrm{He}_i, \tag{2}$$

$$\mathrm{He}_n V_p + \mathrm{He}_i \rightleftharpoons \mathrm{He}_{n+1} V_p, \tag{3}$$

$$\mathrm{He}_n V_p + V \rightleftharpoons \mathrm{He}_n V_{p+1}, \tag{4}$$

$$I + V \rightleftharpoons 0, \tag{5}$$

$$I_n + I \rightleftharpoons I_{n+1}, \tag{6}$$

$$I_n + I_2 \rightleftharpoons I_{n+2}, \tag{7}$$

$$I_n + V \rightarrow I_{n-1}, \tag{8}$$

$$V_n + I \rightarrow V_{n-1}. \tag{9}$$

Recombination between defects and their antidefects can also occur—that is, between self-interstitials and vacancies—either isolated or in clusters. In the reactions above, $\mathrm{He}_n V_p$ clusters are defined independently of the specific positions of the n He atoms.

Table I summarizes the reactions which are taken into account in the present simulations and the values used for the corresponding binding energies as obtained from *ab initio* calculations.[10,12] The exact atomic structure of these $\mathrm{He}_n V_p$ clusters can be found in Ref. 12. For larger clusters, an extrapolation law was used to calculate the binding energies, as is done in other works.[10,14] In the present model, a substitutional He atom can become mobile; i.e., it can go at an interstitial site, through two possible mechanisms: the Frank-Turnbull[15] and kick-out[16] mechanisms. The first one occurs when a substitutional He moves to an interstitial site, leaving a vacancy behind [see Eq. (1)]. The second one occurs when a self-interstitial displaces a HeV into an interstitial site, corresponding to Eq. (2). *Ab initio* calculations[12] show that He can also diffuse in Fe by the migration of $\mathrm{He}V_2$ complexes. However, the migration energy involved in this

TABLE I. Defect-defect binding energies corresponding to the DFT-GGA calculations presented in Refs. 10 and 12. The binding energy of a reaction $A+B \leftrightarrows C$ is defined as $E_b=E_A^f+E_B^f-E_C^f$, where E_A^f, E_B^f, and E_C^f are the formation energies of A, B, and C, respectively. All values correspond to constant-pressure calculations performed on supercells containing 128 atomic sites.

Reaction	E_b (eV)	Reaction	E_b (eV)
$V+V \leftrightarrows V_2$	0.30		
$V_2+V \leftrightarrows V_3$	0.37		
$V_3+V \leftrightarrows V_4$	0.62		
$I+I \leftrightarrows I_2$	0.80	$\mathrm{He}_i+\mathrm{He}_i \leftrightarrows \mathrm{He}_2$	0.43
$I_2+I \leftrightarrows I_3$	0.92	$\mathrm{He}_2+\mathrm{He}_i \leftrightarrows \mathrm{He}_3$	0.95
$I_3+I \leftrightarrows I_4$	1.64	$\mathrm{He}_3+\mathrm{He}_i \leftrightarrows \mathrm{He}_4$	0.98
$\mathrm{He}_i+V \leftrightarrows \mathrm{He}V$	2.30	$\mathrm{He}V+I \leftrightarrows \mathrm{He}_i$	3.60
$\mathrm{He}V+V \leftrightarrows \mathrm{He}V_2$	0.78	$V_2+\mathrm{He}_i \leftrightarrows \mathrm{He}V_2$	2.85
$\mathrm{He}V_2+V \leftrightarrows \mathrm{He}V_3$	0.83	$V_3+\mathrm{He}_i \leftrightarrows \mathrm{He}V_3$	3.30
$\mathrm{He}V_3+V \leftrightarrows \mathrm{He}V_4$	1.16	$V_4+\mathrm{He}_i \leftrightarrows \mathrm{He}V_4$	3.84
$\mathrm{He}_2+V \leftrightarrows \mathrm{He}_2V$	3.71	$\mathrm{He}V+\mathrm{He}_i \leftrightarrows \mathrm{He}_2V$	1.84
$\mathrm{He}_2V+V \leftrightarrows \mathrm{He}_2V_2$	1.61	$\mathrm{He}V_2+\mathrm{He}_i \leftrightarrows \mathrm{He}_2V_2$	2.75
$\mathrm{He}_2V_2+V \leftrightarrows \mathrm{He}_2V_3$	1.04	$\mathrm{He}V_3+\mathrm{He}_i \leftrightarrows \mathrm{He}_2V_3$	2.96
$\mathrm{He}_2V_3+V \leftrightarrows \mathrm{He}_2V_4$	1.32	$\mathrm{He}V_4+\mathrm{He}_i \leftrightarrows \mathrm{He}_2V_4$	3.12
$\mathrm{He}_3+V \leftrightarrows \mathrm{He}_3V$	4.59	$\mathrm{He}_2V+\mathrm{He}_i \leftrightarrows \mathrm{He}_3V$	1.83
$\mathrm{He}_3V+V \leftrightarrows \mathrm{He}_3V_2$	1.85	$\mathrm{He}_2V_2+\mathrm{He}_i \leftrightarrows \mathrm{He}_3V_2$	2.07
$\mathrm{He}_3V_2+V \leftrightarrows \mathrm{He}_3V_3$	1.8	$\mathrm{He}_2V_3+\mathrm{He}_i \leftrightarrows \mathrm{He}_3V_3$	2.91
$\mathrm{He}_3V_3+V \leftrightarrows \mathrm{He}_3V_4$	1.57	$\mathrm{He}_2V_4+\mathrm{He}_i \leftrightarrows \mathrm{He}_3V_4$	3.16
$\mathrm{He}_4+V \leftrightarrows \mathrm{He}_4V$	5.52	$\mathrm{He}_3V+\mathrm{He}_i \leftrightarrows \mathrm{He}_4V$	1.91
$\mathrm{He}_4V+V \leftrightarrows \mathrm{He}_4V_2$	2.3	$\mathrm{He}_3V_2+\mathrm{He}_i \leftrightarrows \mathrm{He}_4V_2$	2.36
$\mathrm{He}_4V_2+V \leftrightarrows \mathrm{He}_4V_3$	2.03	$\mathrm{He}_3V_3+\mathrm{He}_i \leftrightarrows \mathrm{He}_4V_3$	2.57
$\mathrm{He}_4V_3+V \leftrightarrows \mathrm{He}_4V_4$	1.97	$\mathrm{He}_3V_4+\mathrm{He}_i \leftrightarrows \mathrm{He}_4V_4$	3.05

mechanism is relatively high—1.1 eV—in comparison to the one of He_i. Moreover, with a V-HeV binding energy of 0.78 eV, HeV_2 dissociates rapidly at temperatures above room temperature. Therefore, this migration mechanism is very unlikely and was not included in our model.

The atomistic processes considered here can be described within a rate equation formalism. Thus, taking into account their diffusion and their possible reactions with other defects, the evolution of mobile defects can be modeled by a set of one-dimensional (1D) spatial diffusion-reaction equations. On the other hand, immobile clusters He_nV_p and I_n clearly follow a Markovian chain process and their kinetics can then be described by a master equation, as is done in Ref. 17. Forward and backward rate constants corresponding to the reactions shown in Table I were calculated following Refs. 18 and 19, respectively. In order to account for He desorption first-order boundary conditions were used, assuming that the flux of He_i atoms at the surface is proportional to the He_i concentration and only limited by diffusion; i.e., no extra barrier is required. The same type of boundary conditions was used for I, V, and I_2 defects. It has been checked that dislocations play a very minor role in the conditions studied here. Therefore, in our model the surface is the only sink for I, V, and I_2.

Using the kinetic model and the *ab initio* data described above we have simulated the desorption experiments carried out by Vassen *et al.*[20] In these experiments the thermal desorption of helium homogeneously implanted in iron was studied. The purpose of this experiment was to obtain basic information about He diffusion mechanisms in α-Fe. The released fraction of helium was measured during isothermal annealing for various temperatures, foil thicknesses, and initial He concentrations: (a) 559 K, 2.5 μm, 1.39 atoms ppm, (b) 577 K, 20.6 μm, 0.013 atoms ppm, and (c) 667 K, 2.6 μm, 0.109 atoms ppm. In order to model these experiments the initial concentration of point defects generated by the irradiation process was determined using TRIM.[21] These simulations indicate that on the average 200 I-V pairs were generated per implanted He. Considering the defects present after irradiation—i.e., He_i, I, and V—we first simulated the evolution of the system at room temperature (300 K) until a steady state is reached. Indeed, interstitial atoms (I and He_i) are highly mobile and can migrate even at low temperature.[10,12] Our simulations show that after a steady state is reached at room temperature, most of the He_i atoms have recombined with vacancies and are at substitutional sites. Simulation results also reveal that a very small amount of He_2V complexes are formed by the reaction $\mathrm{He}V+\mathrm{He}_i \rightarrow \mathrm{He}_2V$. As expected, simulations confirm that most vacancies persist as isolated defects at room temperature, due to their relatively high migration energy. Only a very small fraction is trapped in the He_2V clusters. Finally, our model predicts that at room temperature, most self-interstitial atoms that are created during implantation diffuse and agglomerate into small immobile I_n clusters containing less than 15 interstitials. In summary, at 300 K, the main defects are HeV, V, and I_n. After the 300 K calculation, He desorption during isothermal annealing was simulated for the experimental conditions described in Ref. 20. In Fig. 1(a) we present the simulated released fraction of implanted He for isothermal annealings at temperatures of 559, 577, and 667 K. The experimental data obtained by Vassen *et al.* are also reported for comparison. Clearly, Fig. 1(a) shows that the model just described cannot quantitatively reproduce the released fraction of helium measured experimentally.

As mentioned above, after implantation all He atoms are at substitutional sites, while all self-interstitials are in immobile clusters and vacancies are mostly isolated. Since self-interstitial species diffuse much faster than vacancies, in the time scale of the experimental observations He diffusion is likely to be governed by the energetic properties of He-V complexes and the migration of vacancies. Thus, any modification of these properties directly affects He diffusion. Consequently, the migration energy of vacancies and the binding energy of a vacancy to He_i and to HeV were modified until good agreement with the experimental data was reached for all conditions described in Ref. 20. This was obtained for an effective vacancy migration energy of 0.83 ± 0.08 eV, instead of 0.67 eV, and effective binding energies of 1.78 ± 0.02 eV and 0.54 ± 0.06 eV instead of 2.30 and 0.78 eV for V-He_i and V-HeV, respectively. With these fitted values of vacancy parameters, the model reproduces very well the different experimental phases of He desorption over several orders of magnitude in time and for very different conditions of temperature, sample depth, and He concentration, as shown in Fig. 1(b).

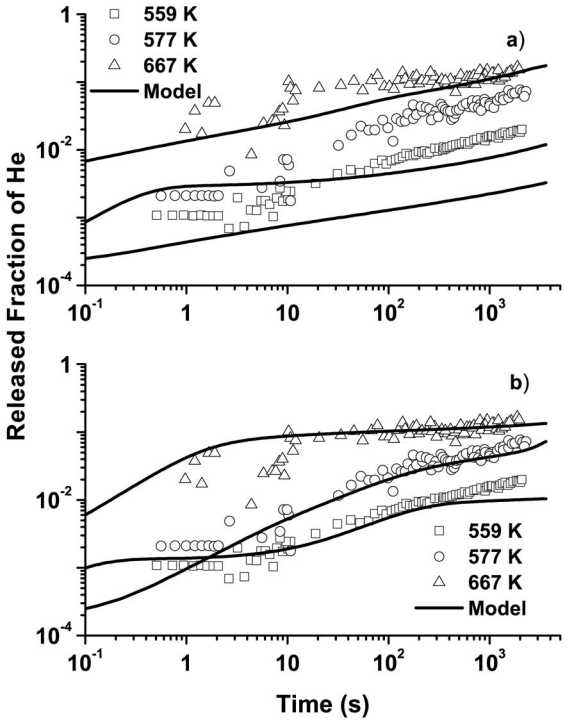

FIG. 1. Comparison between the experimental desorption data of Ref. 20 (open symbols) and simulations (solid lines) with (a) input data from *ab initio* calculations and (b) fitted values of the vacancy migration energy and V-He$_i$ and V-HeV binding energies.

Analyzing existing experimental data, Hardouin-Duparc and Barbu[22] have pointed out that two different values are obtained experimentally for the vacancy migration energy in Fe. A set of experiments reports values around 1.3 eV while another group of experiments[5,22,23] provide a value of around 0.6 eV. The difference in these values is commonly attributed to the presence of impurities. Similarly, Hudson *et al.* have shown that solute atoms can dramatically reduce the mobility of self-interstitial clusters above a critical concentration of trapping centers.[24] The fitted value found in the present work for the effective vacancy migration energy in comparison to that predicted by *ab initio* calculations suggests that vacancies interact with trapping impurities. *Ab initio* calculations[25–27] show that this impurity could be carbon, since it forms a C-V complex with a positive binding energy. On the other hand, the fitted value found for the dissociation energy of HeV—i.e., 1.78+0.06=1.84 eV—is significantly lower than the one predicted by *ab initio* calculations, 2.36 eV, and it is in good agreement with the one obtained experimentally by Vassen *et al.*:[20] namely, 1.4±0.3 eV. Hardouin-Duparc *et al.*[22] have also pointed out that values between 1.6 and 2.0 eV can be found experimentally[5] for the formation energy of vacancies in Fe, with a lower formation energy for higher impurity content. Notice that, by definition, the binding energy of a vacancy to a He-V complex is a function of its formation energy. Thus, a lower value in the vacancy formation energy would also result in lower V-He$_i$ and V-HeV binding energies. Therefore, a plausible explanation for the discrepancy between the model with *ab initio* values corresponding to He in pure bcc Fe and the experimental data is the lack of impurities in the initial model. These results show that, if one or several limiting processes are not included in the model, the advantage of density functional theory (DFT) accuracy could be lost. This suggests that a DFT investigation should be, at least partially, guided by experiment. The values obtained from the fit should then be interpreted as effective values for vacancy migration energy and dissociation energies of He-V clusters in the presence of impurities. Since carbon is always present in Fe and since it strongly interacts with vacancies as confirmed by the large binding energy found in *ab initio* calculations, this impurity is the most likely candidate for this effect. It is important to note that, even though good results can be obtained by reevaluating some of the *ab initio* parameters, in a more rigorous approach one should explicitly include the formation of He-V-C complexes and therefore extend the *ab initio* database.

It is now possible to study in detail the role of the different migration mechanisms of He during desorption. Notice from the experimental data in Figs. 1(a) and 1(b) that three different regimes can be defined: an initial plateau (not observed at the highest temperature), followed by a rapid He release and a slower desorption rate at later times. All these regimes can be resolved with the model described above [see Fig. 1(b)]. Analyzing the calculations we can observe that each of these stages is actually dominated by a different He migration mechanism. For instance, for the case of 559 K, simulations show that during the first 10^{-2} s of annealing, the formation of mobile He$_i$ atoms, which are responsible for He desorption, is highly dominated by the kick-out mechanism.

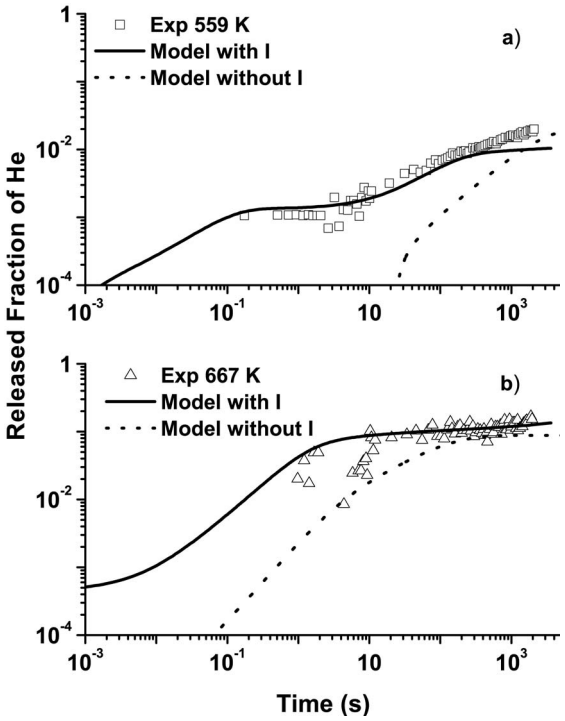

FIG. 2. Released fraction of He as a function of time for (a) 559 K and (b) 667 K. Open symbols are the experimental results from Vassen *et al.* (Ref. 20), and lines are calculations with (solid) and without (dashed) self-interstitial atoms.

This indicates that He atoms that are initially at substitutional sites are kicked out from their sites by a large flux of self-interstitials. According to simulations, these self-interstitials arise from the dissolution of small I_n clusters comprising fewer than five atoms. This stage cannot be observed experimentally since it takes place at very short times. Calculations show that after this short period of fast desorption, the I_n clusters left do not dissociate, giving rise to an abrupt decrease of the He_i formation rate. Hence, the initial plateau that is observed experimentally at short times in the He desorption curves obtained at 559 K and 577 K [see Fig. 1(b)] is due to a very fast generation of He_i atoms by the kick-out mechanism occurring at the early stages of annealing, followed by a strong reduction of the He_i formation rate. After 1 s annealing and up to $t \simeq 750$ s, the formation of mobile He_i is governed by the Frank-Turnbull mechanism, which corresponds to the increased desorption rate observed at intermediate times. According to the model, for long annealing times, He is found predominantly in He_nV_p clusters. Therefore, the emission of mobile He_i, and thus desorption, is mainly due to the dissociation of these complexes. Since they are relatively stable, this regime results in a slower desorption rate, as can be observed experimentally at all temperatures. These results are in agreement with the conclusions of Vassen *et al.*[20]

To evidence the role of self-interstitial clusters—formed at room temperature—in He desorption, we simulated He desorption at 559 and 667 K without including self-interstitials. Results are reported in Fig. 2 and compared to experimental data and the full model. Clearly, when self-interstitials are neglected, the model fails to predict the different regimes of He desorption. In particular, the initial plateau that is observed experimentally at 559 K is not reproduced. This shows that small interstitial clusters $I_{n \leqslant 5}$ influence the whole evolution of He desorption even though they dissolve in the early stages of annealing.

In summary, we have developed a rate theory model for He diffusion in Fe based primarily on *ab initio* results for defect energetics. Good agreement between calculations and experimental results could be obtained by using effective values for the vacancy migration and V-He_i and V-HeV binding energies. The values found could be explained by invoking the presence of impurities in the experimental samples. One likely candidate, considering experimental observations and *ab initio* calculations, is carbon. In addition, our model reveals that several mechanisms govern He diffusion during isothermal annealing. In particular, the model shows that self-interstitial clusters play a fundamental role in the diffusion of He in irradiated Fe. Further experiments on very high-purity samples would contribute validation of the model presented here as well as the parameters used.

C. J. Ortiz thanks EC for its support, project No. TOOL-SPIE FI60–012648. This work was partially funded by EC, IP Project No. PERFECT FI60-CT-2003-0508840 and EFDA. M. J. C. thanks the Spanish Ministerio de Educacion y Ciencia for support under the Ramon y Cajal program.

*Electronic address: christophe.ortiz@ua.es

[1] R. Andreani, E. Diegele, R. Laesser, and B. van der Schaaf, J. Nucl. Mater. **329**, 20 (2004).
[2] L. K. Mansur, E. H. Lee, P. J. Maziasz, and A. P. Rowcliffe, J. Nucl. Mater. **633**, 141 (1986).
[3] W. D. Wilson and C. L. Bisson, Radiat. Eff. **25**, 197 (1975).
[4] R. H. J. Fastenau, L. M. Caspers, and A. van Veen, Phys. Status Solidi A **34**, 277 (1976).
[5] P. Ehrhart, P. Jung, H. Schultz, and H. Ullmaier, *Numerical Data and Functional Relationships in Science and Technology*, edited by H. Ullmaier, *Atomic Defects In Metals*, Landolt-Börnstein, New Series, Group III Condensed Matter, Vol. 25, Pt. 3 (Springer, Berlin, 1991).
[6] H. Trinkaus and B. N. Singh, J. Nucl. Mater. **323**, 229 (2003).
[7] H. L. Heinisch, B. N. Singh, and S. I. Golubov, J. Nucl. Mater. **276**, 59 (2000).
[8] M. J. Caturla, N. Soneda, E. Alonso, B. D. Wirth, T. D. de la Rubia, and J. M. Perlado, J. Nucl. Mater. **276**, 13 (2000).
[9] C. Domain, C. S. Becquart, and L. Malerba, J. Nucl. Mater. **335**, 121 (2004).
[10] C. C. Fu, J. Dalla Torre, F. Willaime, J.-L. Bocquet, and A. Barbu, Nat. Mater. **4**, 68 (2005).
[11] B. Sadigh, T. J. Lenosky, S. K. Theiss, M.-J. Caturla, T. Diaz de la Rubia, and M. A. Foad, Phys. Rev. Lett. **83**, 4341 (1991).
[12] C. C. Fu and F. Willaime, Phys. Rev. B **72**, 064117 (2005).
[13] T. Seletskaia, Y. Osetsky, R. E. Stoller, and G. M. Stocks, Phys. Rev. Lett. **94**, 046403 (2005).
[14] A. Hardouin-Duparc, C. Moingeon, N. Smetniansky-de-Grande, and A. Barbu, J. Nucl. Mater. **302**, 143 (2002).
[15] F. C. Frank and D. Turnbull, Phys. Rev. **104**, 617 (1956).
[16] U. Gösele, W. Frank, and A. Seeger, Appl. Phys. **23**, 361 (1980).
[17] C. J. Ortiz, P. Pichler, T. Fühner, F. Cristiano, B. Colombeau, N. E. B. Cowern, and A. Claverie, J. Appl. Phys. **96**, 4866 (2004).
[18] T. R. Waite, Phys. Rev. **107**, 463 (1957).
[19] P. Pichler, *Intrinsic Point Defects, Impurities, and Their Diffusion in Silicon* (Springer, Berlin, 2004).
[20] R. Vassen, H. Trinkaus, and P. Jung, Phys. Rev. B **44**, 4206 (1991).
[21] J. P. Biersack and L. G. Haggmark, Nucl. Instrum. Methods **174**, 257 (1980).
[22] A. Hardouin-Duparc and A. Barbu, in *Microstructure Evolution During Irradiation*, edited by I. M. Robertson *et al.*, MRS Symposia Proccedings No. 439 (Materials Research Society, Pittsburgh, 1997), p. 509.
[23] P. Moser, C. Corbel, P. Lucasson, and P. Hautojarvi, Mater. Sci. Forum **15-18**, 925 (1987).
[24] T. S. Hudson, S. L. Dudarev, and A. Sutton, in *Royal Society: Mathematical, physical and engineering sciences*, edited by the Royal Society of London (Royal Society of London, London, 2004), Vol. 460, pp. 2457–2475.
[25] C. Domain, C. S. Becquart, and J. Foct, Phys. Rev. B **69**, 144112 (2004).
[26] L. Joly *et al.* (unpublished).
[27] C. J. Först, J. Slycke, K. J. Van Vliet, and S. Yip, Phys. Rev. Lett. **96**, 175501 (2006).